American Journal of Materials Synthesis and Processing
2020; 5(1): 1-9
http://www.sciencepublishinggroup.com/j/ajmsp
doi: 10.11648/j.ajmsp.20200501.11
ISSN: 2575-2154 (Print); ISSN: 2575-1530 (Online)

A Laboratory-Based Case Study to Remove MTBE from Contaminated Water with Pure-WO_3 and Nano-WO_3 Catalysts Loaded with Ru and Pt

Saleh Hamad Al-Sharidi*, Husin Sitepu

Research and Development Center, Saudi Aramco, Dhahran, Saudi Arabia

Email address:

saleh.sharidi@aramco.com (S. H. Al-Sharidi)

*Corresponding author

To cite this article:

Saleh Hamad Al-Sharidi, Husin Sitepu. A Laboratory-Based Case Study to Remove MTBE from Contaminated Water with Pure-WO_3 and Nano-WO_3 Catalysts Loaded with Ru and Pt. *American Journal of Materials Synthesis and Processing.* Vol. 5, No. 1, 2020, pp. 1-9.
doi: 10.11648/j.ajmsp.20200501.11

Received: May 13, 2020; **Accepted**: June 15, 2020; **Published**: September 14, 2020

Abstract: This article describes a laboratory-based case study to remove methyl tertiary butyl ether (MTBE) from contaminated water with tungsten oxide (WO_3) catalysts loaded with ruthenium (Ru) and platinum (Pt) metals. Characterization of the synthesized catalysts were conducted by using the: (i) X-ray powder diffraction (XRD) data for the purity, (ii) visible light reaction condition for MTBE, (iii) solid-phase micro-extraction (SPME) technique incorporated with gas chromatography mass spectrometry (GC-MS) to assist the MTBE photo-oxidation process, (iv) catalyst syntheses from different concentrations of Ru in WO_3, nano-WO_3, Pt in nano-WO_3, and (v) formation of byproducts during photocatalytic degradation of MTBE by using the GC-MS. The results revealed that the catalysts mainly consists of WO_3 phase and there is no additional peaks from the metals, indicating that the Ru and Pt metals are well dispersed on WO_3. Approximately 96% to 99% of the MTBE removal can quickly and accurately be achieved with a nanostructured WO_3 catalyst loaded with Pt under visible light radiation between 2.5h and 3h. Moreover, with a nanocomposite WO_3 catalyst loaded with Pt, photocatalytic MTBE removal is higher than with the pure WO_3 catalyst loaded with Ru, and the pure nanostructured and micron-sized WO_3. Finally, the formation of byproducts during the MTBE photocatalytic degradation revealed that the MTBE degradation essentially proceeds via formation of formic acid and 1, 1-dimethylethyl ester before its complete degradation.

Keywords: MTBE Photocatalytic Degradation, Ru and Pt Loaded in Pure-WO_3 and nano-WO_3 Catalysts, XRD, GC-MS, Visible Light Radiation

1. Introduction

The unexpected accidental fuel leakage during storage and transportation is one of the concerns raised by the World Health Organization, and therefore, there are many studies have been conducted to remove methyl tertiary butyl ether (MTBE) from contaminated water. To improve the octane number and increase the gasoline combustion efficiency, MTBE as the oxygenated chemical has been used by many research groups [1-3 and the references therein]. Additionally, MBTE has been widely used as a gasoline additive by supplying extra oxygen during the combustion process. Therefore, carbon monoxide and volatile organic carbon emissions from internal combustion engines and air pollution can be reduced. Nevertheless, human and environmental health concerns have been raised due to-mainly-accidental fuel leakage [4-5]. The United States Environmental Protection Agency put advisory regulations of 20 to 40 ppb [6, 7] in drinking water and banned MTBE.

It was difficult to remove the MTBE from contaminated water by using many different techniques such as air stripping, photo-oxidation, granular activated carbon or bio-treatment, and therefore, the heterogeneous catalysts combined with photo-oxidation for the removal of MTBE from water resources was studied by many research groups. Semiconducting metal oxides was used by Seddigi et al. [8 and the references therein] to investigate the MTBE photocatalytic degradation in water. They described that

1. both titanium dioxide (TiO_2) and zinc oxide (ZnO) were effective photo catalysts in MTBE remediation by using artificial ultra violet (UV) radiation,
2. UV TiO_2 and ZnO were used with the visible light in the photocatalytic process instead of using the energy source of,
3. a simple single semiconductor catalyst is obviously not effective to remove waste waters containing toxic chemicals,
4. it is nevertheless a promising result if a doped catalyst that works in the visible light is taken with great care,
5. use the solar spectrum for the degradation of complex molecules to measure the photocatalytic action of the mixed oxide doped photocatalysts, and
6. optimize the effective photocatalytic reaction parameters to obtain the efficiencies of the contaminants' photocatalytic degradation.

After treating the MBTE in the packed bed reactor, Alfonso-Gordillo et al. [9 and the references therein] indicated that the influent toxicity was significantly reduced. Therefore, to remove MTBE from high strength MTBE polluted water, this approach may be a promising alternative to existing technologies.

The objective of this study is to remove MTBE from contaminated water with tungsten oxide (WO_3) catalysts loaded with ruthenium (Ru) and platinum (Pt) metals-a laboratory-based case study. The specific objectives of the present study were to:

Study the synthesis of noble metals (Ru/Pt) loaded on pure-WO_3, nano-WO_3, and Pt in nano-WO_3.

Determine the purity of the synthesized catalysts by X-ray powder diffraction (XRD) diffractometer and its software.

Develop visible light reaction condition for MTBE.

Investigate the MTBE photo-oxidation study.

Evaluate the formation of byproducts during photocatalytic degradation of MTBE by using the gas chromatography mass spectrometry (GC-MS).

2. Experimental

To fulfill these objectives, in the present study-the authors have: (i) prepared the MTBE samples, (ii) synthesized WO_3 in sodium tungstate (Na_2WO_4), (iii) synthesized the noble metals (Ru/Pt) loaded on both pure-WO_3 and on nano-WO_3 catalysts, (iv) determine the purity of the synthesized catalysts by XRD and its software, (v) investigated the catalysts by photo-oxidation reactor, and (vi) evaluate the efficiency of the catalysts. They are described in turn next.

2.1. MTBE Samples

The MTBE stock solution of 1,000 ppb was prepared by dissolving 0.00025 g of MTBE in 2.0 L of water, and then 100 ml of 1,000 ppb MTBE stock solution was added in 1 L to prepare 100 ppb MTBE stock solution that was used for the reaction. The study utilized a visible light in a 500 ml reactor and the lamp introduced an immersion well photochemical reactor made of Pyrex glass equipped with a magnetic stirring bar, a water circulating jacket, and an opening for the supply of gases. The preparation of the photo-oxidation experiments and the synthesized catalyst procedures were described by Sharidi [10, 11].

2.2. Synthesizing WO_3 in Na_2WO_4

Dissolve Na_2WO_4 (6.6 g, 0.2 mole) in 100 mL of double distilled water (DDW), then the acidification was conducted by adding hydrochloric acid to get a pH of 1 to obtain a white precipitate, and dissolved by adding oxalic acid (0.4 g in 30 mL DDW, 0.1 mole). As a result, a transparent solution was obtained. The solutions were transferred into a 100 mL Teflon-lined stainless steel autoclave and maintained at 180°C for 24 hours to get the final product.

2.3. Synthesis of Noble Metals (Ru/Pt) Loaded on Pure-WO_3 and Nano-WO_3 Catalysts

The photo deposition of the Ru loaded on the WO_3 was prepared by mixing 500 mg of WO_3 and 100.0 mL of distilled water in a beaker. Then, 2.5 mg of Ru was added to the beaker. After that, the solution bubbled with nitrogen for 30 minutes to remove the excess of O_2 while stirring slowly. Then, 5.0 mL of methanol was added. The solution was then transferred to a reactor and radiated by a lamp for 6 hours while stirring. After that, co-catalyst Ru/WO_3 was centrifuged for 30 minutes. The solid product was dried and the catalyst was calcinated at ~700°C in a furnace. Following the same procedure, the Pt/WO_3 was prepared. The procedures used were to:

Assess the treatability of water contaminated by MTBE.

Develop visible light reaction condition for the MTBE and SPME technique incorporated with GC-MS in assisting the study of the MTBE photo-oxidation.

Synthesize 0.5 wt% of Ru, 1.0 wt% of Ru, 1.5 wt% of Ru, 2.0 wt% of Ru, and 2.5 wt% of

Ru in pure WO_3,

Pt in both pure-WO_3 and nano-WO_3 and

Determine MTBE degradation and hydrocarbon byproducts from photo-oxidation.

2.4. Determination of Purity of the Synthesized Catalysts by XRD Diffractometer and Its Software

Sitepu et al. [12] described that to achieve fine particle size and adequate intensity reproducibility, the as-received powders (i) should manually milled in an agate mortar for several minutes, and subsequently mounted them into the XRD sample holder by back pressing [12-14]. In this paper, the conditions of the XRD data collection is given in Table 1. The measured XRPD data was conducted with a PANalytical X′PERT XRD diffractometer with copper X-ray tube. To identify the measured XRD data, the software package PANalytical High Score Plus (X'Pert HighScore Plus Version 4.8 PANalytical Inc.) [15], combined with the International Center for Diffraction Data (ICDD) of the Powder Diffraction File (PDF-4+) database of the standard reference materials [16], was used in this paper.

2.5. Photo-Oxidation Reactor

Under visible light illumination, the photocatalytic activities of the samples were evaluated in terms of the MTBE degradation according to the following procedures [10) that are yielded reproducibly results:-

1. Approximately 100 mg of the photo catalyst powder was added to the reactor containing 100 ml of MTBE stock solution, which has the concentration of 100 part per billion (ppb).
2. A halogen lamp was placed in the reactor attached to the water flow cooling system.
3. The mixture was stirred gently, samples were taken at certain intervals;

a) 0 minutes, which is called the first sample, was taken after 0.5h of constant stirring with the lamp turned off.
b) 0.5h or 30 minutes, which is called the second sample, where the lamp was switched on,
c) 1h or 60 minutes, which is called the third sample, where the lamp was switched on,
d) 2h or 120 minutes, which is called the fourth sample, where the lamp was switched on,
e) 3h or 180 hours, which is called the fifth sample, where the lamp was switched on, and
f) 4h or 240 minutes, which is called the six sample, where the lamp was switched on.

Table 1. *The optics and XRD data collection condition [12].*

Name	Description
XRD diffractometer	PANalytical X′PERT PRO MPD
X-ray radiation	Cobalt X-ray tube that was operated at 40 kV and 40 mA Wavelength: $K\alpha_1$ = 1.78901Å, Co $K\alpha_2$ = 1.79290Å, $K\alpha_2/K\alpha_1$ ratio = 0.50
XRD optics	480 mm is diameter of the Bragg-Brentano's measuring circle Automatic mode was used in divergence slit 10 mm used both for irradiated length and specimen length 100 mm is the distance focus to divergence slit
Sample	XRD sample holder has a circular form with the diameter of 20 mm Sample spinner was for all collections
XRD Detector	Position sensitive detector (PSD) X'Celerator 2.12° is the 2θ Bragg-angle's PSD length
XRD Acquisition	2°-70° is the 2θ Bragg-angle's angular range 0.008° is the 2θ Bragg-angle's step size and 9.7282 seconds of the scanning step time

2.6. GC-MS

GC-MS through the use of the SPME technique was used to evaluate the efficiency of the used catalysts. Below shows the experimental procedures conducted in this study

a) keeping the fiber above the liquid level, and retaining 0.17h of the SPME in each vial for collecting the vapors of MTBE with great care,
b) injecting it into the GC-MS instrument with a counting time of approximately 0.15h for the single analysis,
c) collecting the data twice for each samples to ensure the reproducibility of the results,
d) dipping the fiber in water between each data collection, injecting it into the GC-MS, and ensuring that there is no MTBE contamination coming from the previous sample.

2.7. Reproducibility

Scarlett *et al.* [17] described that one of the main sources of error to perform accurately quantitative phase analysis of high quality of high-resolution XRD data by Rietveld method is microabsorption, which is the presence of absorption contrast between phases. In some circumstances, they showed that the microabsorption proves to be challenging. In this paper, the limited amount of the synthesized pure-WO_3 and nano-WO_3 loaded with Ru and nano-WO_3 loaded with Pt catalysts were manually ground in an agate mortar and a pestle for several minutes to achieve fine particle size [12] and eliminate microabsorption effects. To reproduce the results, the sample preparation were carefully repeated-the size distribution of the limited amount of the synthesize catalysts were modified by McCrone micronizing mill in order to achieve inadequate intensity reproducibility [18]. Excellent agreement was obtained between the results of the two experiments (i.e., McCrone mill-micronizing and manually ground in an agate mortar and a pestle techniques); and following to O'Connor et al. [18]-the microabsorption correction was not conducted-in the refinement. The results of the manually ground in an agate mortar and a pestle for several minutes are quoted here as the experimental data of the limited amount of the synthesized pure-WO_3 and nano-WO_3 loaded with Ru and nano-WO_3 loaded with Pt catalysts were superior quality in terms of counting statistics.

3. Results and Discussion

3.1. XRD Phase Identification Results

XRD analysis was carried out to assess the crystallinity of the synthesized catalyst used in the current study [10-11]. Figure 1 shows the XRD phase identification results for the: (i) 2.5 wt% of the Pt in nano-WO_3, and (ii) 2.5 wt% of the Ru in nano-WO_3 catalys. It is clearly seen from Figure 1 that the samples mainly consist of WO_3. The Ru and Pt are not clearly shown at the XRD patterns, indicating that the Ru and Pt are well dispersed on the WO_3.

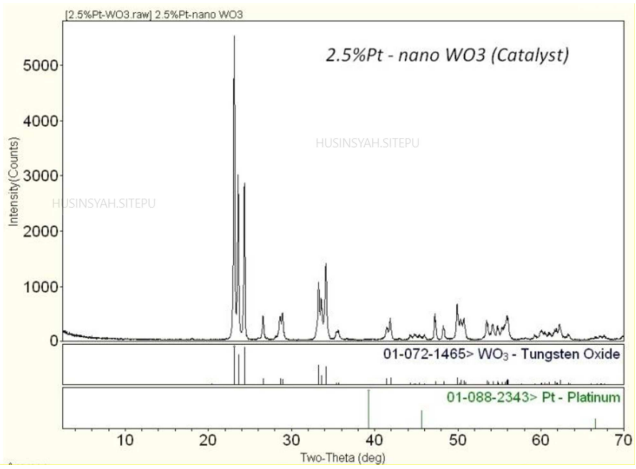

(a) MTBE photo-oxidation by 2.5 wt% of Pt loaded in Nano-WO_3 catalyst.

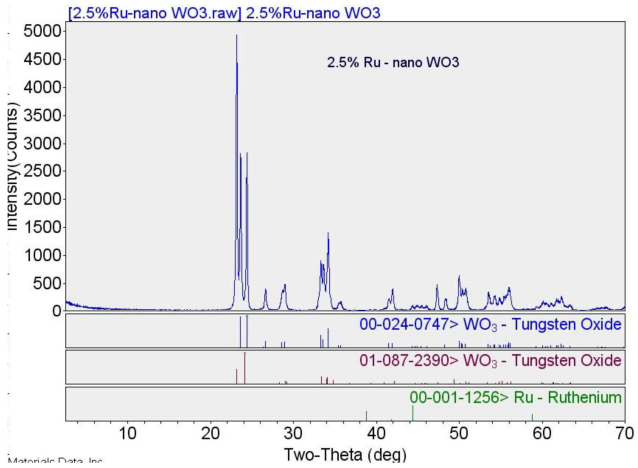

(b) MTBE photo-oxidation by 2.5 wt% of Ru loaded in nano-WO_3 catalyst.

Figure 1. *XRD phase identification results of the synthesized (a) 2.5 wt% of the Pt loaded in nano-WO_3, and (b) 2.5 wt% of the Ru loaded in nano-WO_3 catalysts along with the reference patterns of the identified compounds.*

3.2. MTBE Photo-Oxidation

3.2.1. Pure WO_3

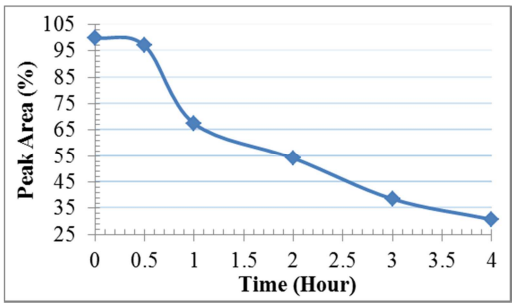

Figure 2. *The degradation of MTBE via pure WO_3 using halogen lamp excitation for 4h.*

The MTBE photo-oxidation was determined by the solid oxide of WO_3 through the halogen lamp excitation for 4h of testing. The catalyst used about 100 mg in the 100 ml stock solution containing 100 ppb MTBE. Figure 2 shows the reduction of MTBE, about 69% after 4h of treatment, with a relative standard deviation of ± 0.2% to 5.9%. The GC-MS diagram of MTBE treated by pure WO_3 for the: (i) 0h, (ii) 0.5h, (iii) 1h, (iv) 2h, (v) 3h, and (vi) 4h yielded a drop in MTBE peak area but no hydrocarbon byproduct was detected, except the MTBE reduction.

3.2.2. MTBE Photo-Oxidation by Ru Loaded with WO_3

Figure 3 depicts the MTBE degradation via 0.5%, 1.0%, 2.0%, and 2.5% of Ru loaded on WO_3 treated by a halogen lamp, with the catalyst weight of 100 mg in 100 mL stock solution containing 100 ppb MTBE. For the 4h treatment, the Ru/WO_3 degraded the MTBE in one systematic trend and the MTBE reduction ranged from 49% to 79%. The results show that the loading of Ru was not much different for the MTBE reduction compared to those of the pure WO_3.

The GC-MS diagram of the treated MTBE by 2.5% Ru/WO_3 for the: (i) 0h, (ii) 0.5h, (iii) 1h, (iv) 2h, (v) 3h, and (vi) 4h yielded the loading of Ru with a not much different reduction of MTBE compared to the pure WO_3. Furthermore, the chromatography of Ru/WO_3 catalysts showed that no hydrocarbon byproducts formed. The reason why the 1 wt% Ru/WO_3 trend is different from other catalysts is not described in this paper and it needs further investigation.

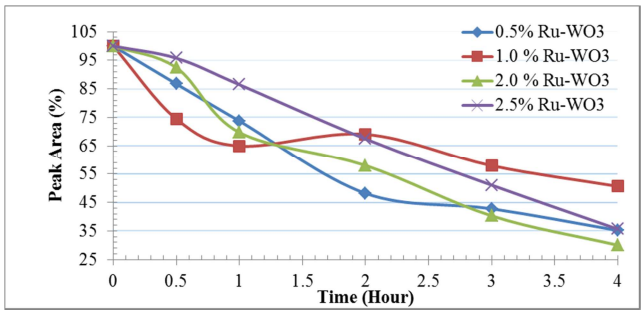

Figure 3. *The MTBE degradation via different concentrations of Ru loaded on the WO_3. The Ru/WO_3 degraded the MTBE in one systematic trend, and the MTBE reduction ranged from 49% to 79% for 4h of treatment.*

3.2.3. MTBE Photo-Oxidation by Ru Loaded on Nano-WO_3

Figure 4 depicts the nano-WO_3 loaded by the Ru catalyst was degraded by the MTBE in one systematic trend and the reduction ranged from 39% to 62% of the MTBE for a 4h treatment duration. The results indicted an increase of Ru, which led to a decrease in the activity of WO_3 and no increase of the MTBE reduction. The GC-MS diagram of the treated MTBE by 2.5% Ru/nano-WO_3 from 0h to 4h under a halogen lamp, with the catalyst weight of 100 mg in a 100 mL stock solution containing 100 ppb MTBE showed neither the degradation of MTBE nor the hydrocarbon byproducts.

3.2.4. Photo-Oxidation of MTBE Via 0.5%, 1.0%, 1.5%, 2.0%, and 2.5% of Pt Loaded on WO_3

Figure 5 shows the variation between the peak area (%) and the time (h) for each of the WO_3 samples loaded with 0.5%, 1.0%, 1.5%, 2.0%, and 2.5% of Pt. From 1h to 3h, it clearly can be seen from Figure 5 that the Pt loaded on the WO_3 degraded the MTBE sharply and increased dramatically. Subsequently, between 3h and 4h, the MTBE treatment increased decimally only and achieved 98% after reaching 4h. Figure 7 illustrates the photo-oxidation of WO_3 loaded with 0.5% Pt to MTBE obtained

from the GC-MS, suggesting that the byproduct of formic acid 1,1-dimethylethyl ester was generated during the oxidation after reaching 1h. While the byproduct increases, the MTBE decreases after reaching 2h of the treatment. Then, after reaching approximately 3h, the MTBE reduced more than 90%. Note that the byproduct also started to decrease after reaching 3h. Additionally, the byproduct was reduced to a trace level after continuous treatment at 4h.

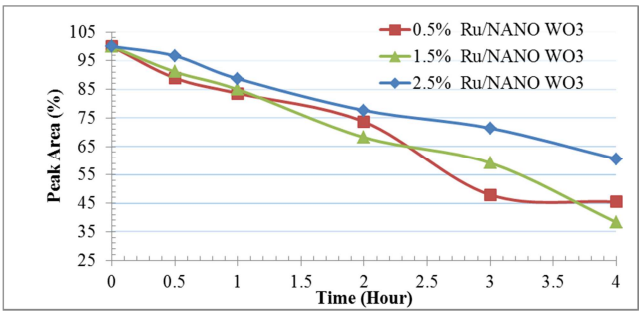

Figure 4. *The MTBE degradation via 0.5%, 1.5%, and 2.5% of Ru loaded on the nano-WO_3. The degradation ranged from 39% to 62% of the MTBE for 4h of treatment. The results indicted an increase of Ru, led to a drop in the activity of WO_3, but no increase in the degradation of the MTBE.*

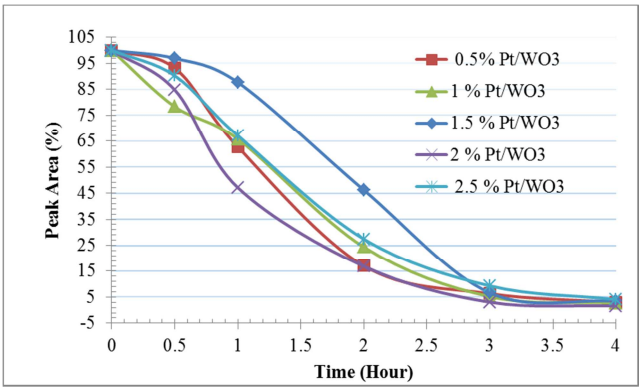

Figure 5. *The MTBE degradation via 0.5%, 1.0%, 1.5%, 2.0%, and 2.5% of Pt loaded on the WO_3. The degradation of the MTBE was very steep and degradation intensified after 1h to 3h, and then after 4h, 98% of the MTBE degradation was achieved.*

3.2.5. MTBE Photo-Oxidation by 0.5%, 1.5%, and 2.5 wt% of Pt Loaded in Nano-WO_3

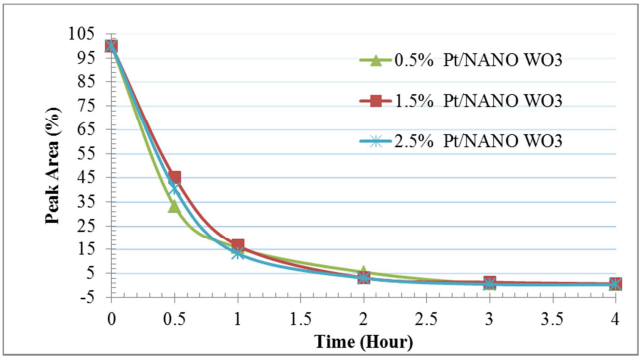

Figure 6. *The degradation of MTBE via different concentrations of Pt loaded on the nano-WO_3 treated by a halogen lamp with catalyst weighing 100 mg in a 100 mL stock solution of 100 ppb MTBE. After 3h of treatment, around 99% degradation of the MTBE was achieved.*

It is the same as Section 3.3.4 above, where the authors conducted the experiment at 4h independently for each catalyst (100 mg) in a 100 mL stock solution containing 100 ppb MTBE. Figure 6 shows the variation between the peak area (%) and the time (h) for each of the nano-WO_3 loaded 0.5%, 1.0%, 1.5%, 2.0%, and 2.5% of Pt. It can be seen from Figure 6 that, when the Pt is loaded on the nano-WO_3, an 85% MTBE degradation was achieved after treating for 1h. Additionally, for all nano-WO_3 loaded with 0.5%, 1.0%, 1.5%, 2.0%, and 2.5% of Pt, 99% of MTBE degradation was achieved after treating for 3h, whereas the byproduct only showed the trace. After treating 3 hours, it can be seen clearly that the byproduct was dramatically reduced from the nano-WO_3 loaded with Pt compared to those of the photo-oxidation of pure WO_3 loaded with Pt at the same treating time. Figure 8 depicts the results of the nano-WO_3 loaded with 0.5% of Pt. It can be seen clearly from Figure 8 that after treating:

0.5h, the MTBE dramatically decreased. Additionally, a trace amount of formic acid 1,1-dimethylethyl ester was produced as a byproduct, and their peak is the highest.

1h, the MTBE continued decreasing. Moreover, the amount of the byproduct, formic acid 1,1-dimethylethyl ester, was considerably produced.

2h, the MTBE continued decreasing, whereas the peak of byproducts increases slightly.

3h, the MTBE continued decreasing and at the same treating time the byproduct started decreasing to a trace amount.

A laboratory-based case study to remove MTBE from contaminated water with WO_3 catalysts loaded with Ru and Pt metals was conducted by preparing five active catalysts using: (i) the starting pure WO_3, and (ii) the synthesized nano-WO_3 to compare the photo-oxidation with those of the catalysts loaded with Ru and Pt metals.

The photo-oxidation of pure WO_3 helped in degrading up to 70% of MTBE from contaminated groundwater. Also, both pure WO_3 loaded with Ru and nano-WO_3 loaded with Ru showed no improvements in degradation of the MTBE. Subsequently, pure WO_3 loaded with Pt dramatically improved the MTBE degradation, which shows the conversion reached 98% after treating for 4h.

For the pure WO_3, approximately 69% of the MTBE degradation was gradually achieved by photo-oxidation in contaminated groundwater. Subsequently, when pure WO_3 was loaded with the Ru metal, it showed no improvement of the MTBE photo-oxidation catalytical reductions. Additionally, when nano-WO_3 catalysts was loaded with the Ru meatal, it showed lower activity surpassed the degradation of MTBE. The demineralization of MTBE by pure WO_3, both WO_3 loaded with Ru, and nano-WO_3 loaded with Ru revealed that: (i) no hydrocarbon byproduct was observed, and (ii) no completed MTBE photo-oxidation was achieved.

When the pure WO_3 was loaded with Pt metal and the nano-WO_3 was loaded with Pt metal, they: (i) exhibited high activity in photo-oxidation reaction, and (ii) achieved 95% to 98% for pure WO_3 loaded with Pt metal, and (iii) achieved 99% MTBE degradations nano-WO_3 loaded with Pt metal.

Additionally, when the pure WO_3 was loaded with Pt metal after treating 0.5h and 1h, the GC-MS: (i) detected the MTBE demineralization, and (ii) observed byproduct formic acid 1,1-dimethylethyl ester. Additionally, when the nano-WO_3 was loaded with Pt metal, 99% of the MTBE reduction was achieved by photo-oxidation suggesting that these were the highest active catalysts in this study. When the pure WO_3 was loaded with Pt metal, it showed high oxidation and reaction time due to generating the redox of OH* and it acts as an oxidizer agent compared to the pure WO_3 loaded with Ru metal. Additionally, when the nano-WO_3 was loaded with Pt metal, it showed higher oxidation of MTBE than that of the results obtained from the pure WO_3 loaded with Pt. When the pure WO_3 was loaded with Pt, the MTBE demineralization pathway through visible light photo-oxidation followed the equation:

$$MTBE \rightarrow \text{formic acid } 1,1-\text{dimethylethyl ester} \rightarrow CO2 + H2O$$

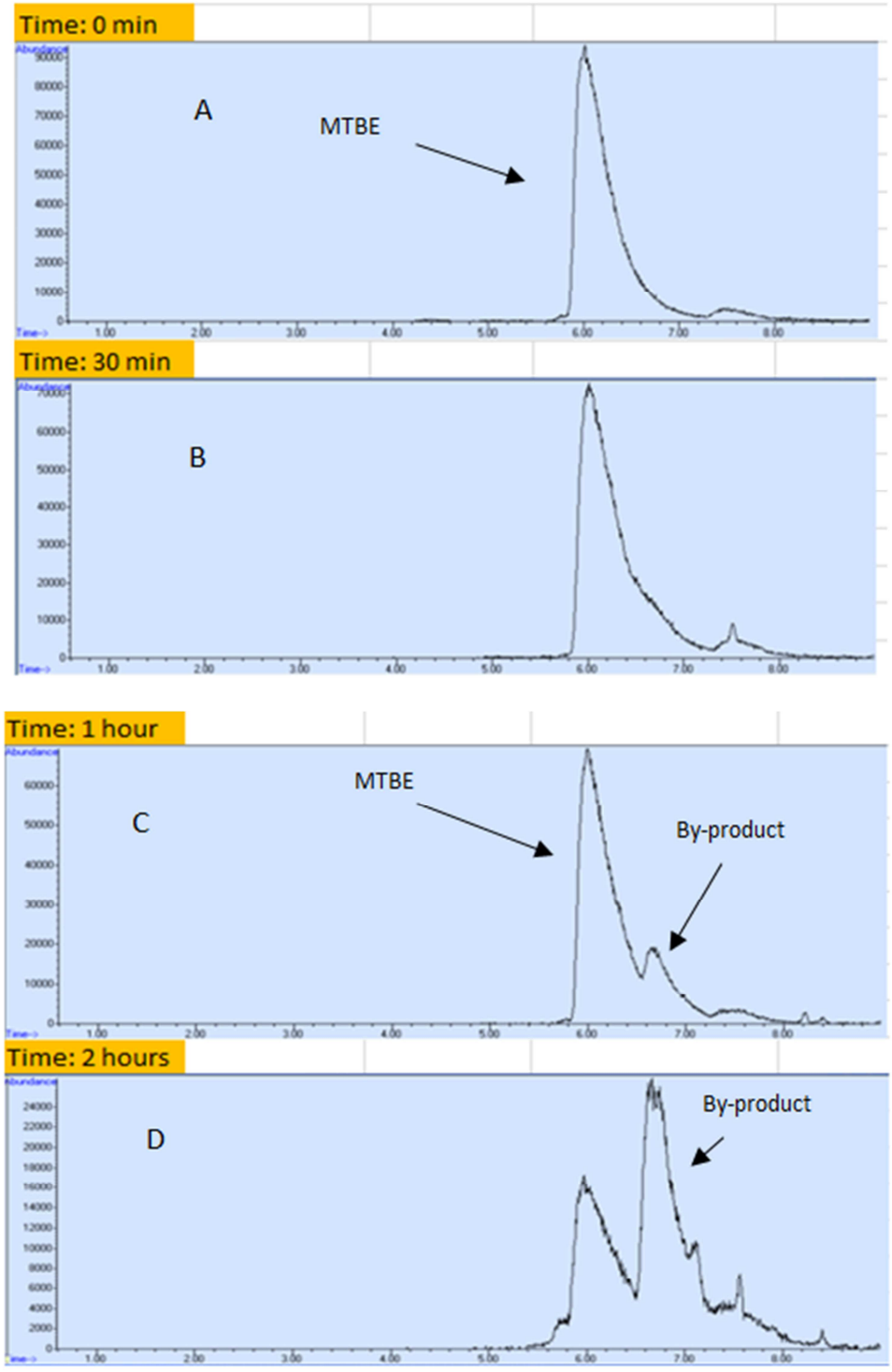

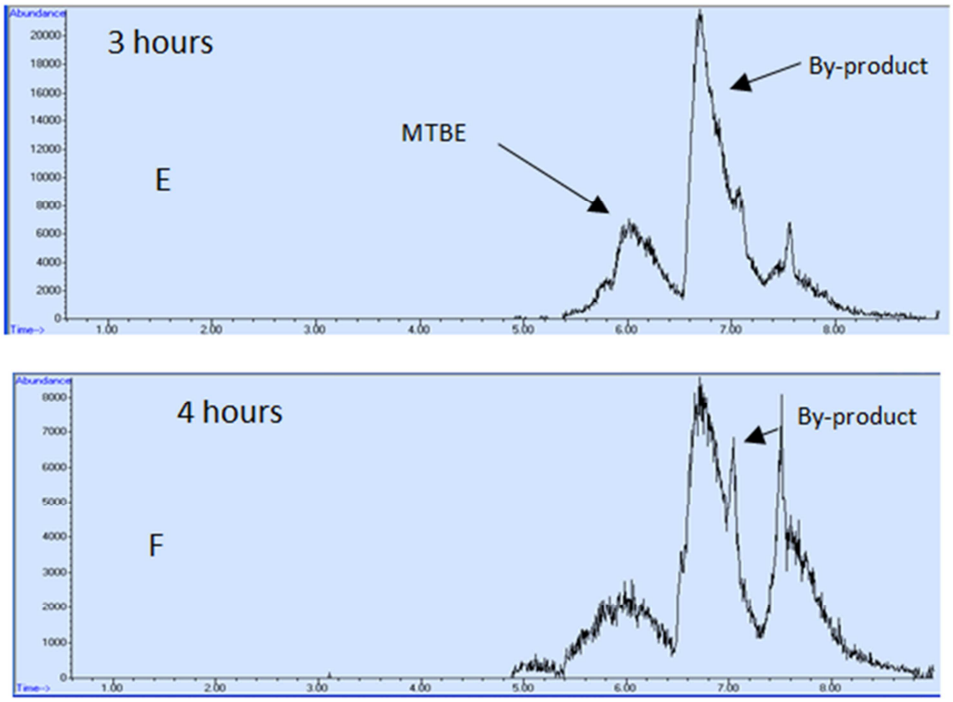

Figure 7. *The GC-MS diagram of MTBE for the pure WO_3 catalyst loaded with 0.5% Pt from 0h to 4h under treatment with a halogen lamp.*

At treating time between 2.5h and 3h, it achieved quickly 96% to 99% of MTBE removal in the presence of nanostructured WO_3 loaded with Pt metal and visible light. Additionally, the pure WO_3 loaded with Pt metal is a superior photocatalytic catalyst than that of the results obtained from: (i) pure WO_3 loaded with Ru, (ii) pure nanostructured WO_3, and (iii) micron-sized WO_3. Moreover, the degradation of MTBE proceeds essentially via intermediate formation of formic acid and 1,1-dimethylethyl ester before its complete mineralization. When the nano-WO_3 was loaded with Pt metal at the visible light condition, it: (i) achieved approximately 99% of the MTBE degradation with traces of a byproduct, and (ii) showed treatability by selected visible light photo-oxidation catalysts. After treating 0.5h, photo-oxidation over the WO_3 and the nano-WO_3 was demonstrated. Additionally, the visible light treatment was faster and generated a HO* redox agent in the nano-WO_3 loaded with Pt. Finally, the synthesized catalyst was identified and confirmed by XRD (Figure 1) and the observed mechanism was proposed based on the mass spectroscopy results (Figures 7 and 8). The findings showed that by using the nano-WO_3 loaded with Pt, 99% of the MTBE treatment can be achieved by photocatalyst.

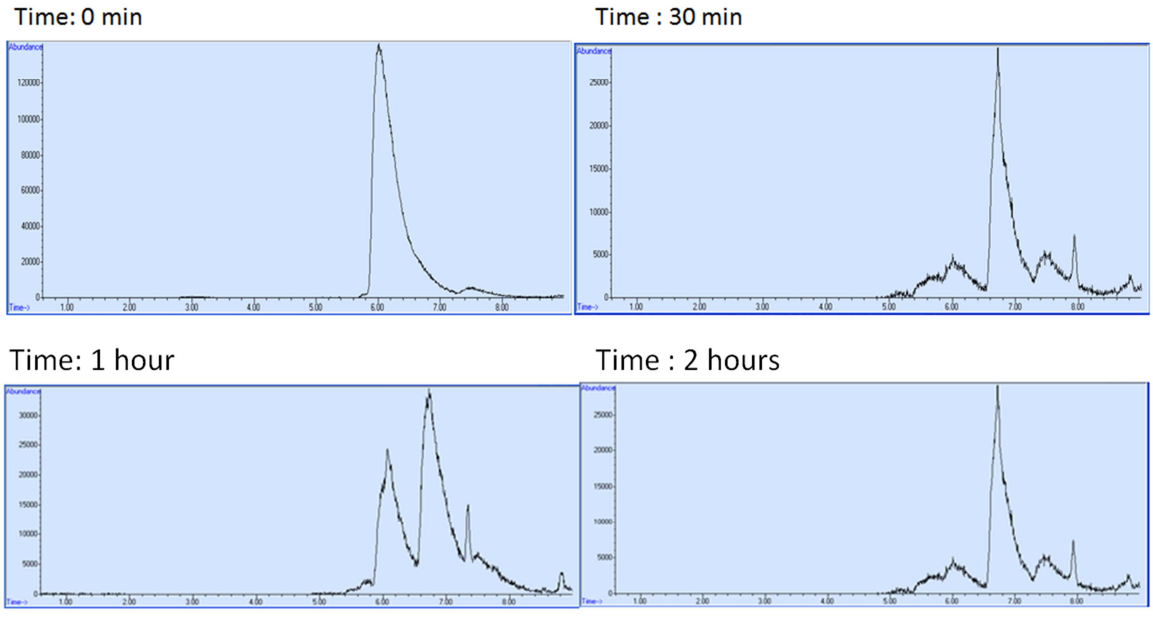

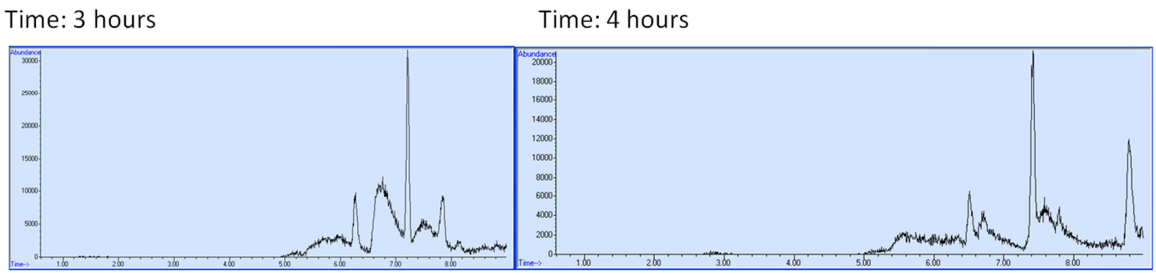

Figure 8. *The photo-oxidation result and the GC-MS diagram for nano-WO_3 catalyst loaded with 0.5% of Pt.*

4. Conclusions

In the present study, the authors remove MTBE from contaminated water with WO_3 catalysts loaded with Ru and Pt metals-a laboratory-based case study conducted by: (i) synthesizing of noble metals (Ru/Pt) loaded on WO_3, and nano-WO_3, Pt in nano-WO_3, (ii) determining the purity of the synthesized catalysts by XRD diffractometer and its software, (iii) developing visible light reaction condition for MTBE, (iv) investigating the MTBE photo-oxidation study, and (v) evaluating the formation of byproducts during photocatalytic degradation of the MTBE. Based on the results, it can be concluded that:

Phase identification results for all of the XRD data sets showed that the synthesized five catalysts with and without loaded metals mainly consist of WO_3. The Ru and Pt are not clearly shown at the XRD patterns, indicating that Ru and Pt are well dispersed on WO_3.

Under visible light radiation between 2.5h and 3h, 96% to 99% MTBE removal can quickly and accurately be achieved when the nanostructured WO_3 catalyst is loaded with Pt.

When the nanocomposite WO_3 catalyst is loaded with Pt, it showed photocatalytic MTBE removal is higher than with the pure WO_3 catalyst loaded with Ru, and the pure nanostructured and micron-sized WO_3.

Byproducts formation during the MTBE photocatalytic degradation revealed that the degradation of MTBE proceeds essentially via the formation of formic acid and 1,1-dimethylethyl ester before its complete degradation.

Acknowledgements

The authors would like to thank the management of Saudi Aramco for permission to publish this article. The support and encouragement of TSD/R&DC management are acknowledged. Thanks are also given to all TSD/R&DC scientists and technicians who helped in this study.

References

[1] Z. S. Seddigi, S. A. Ahmed, S. P. Ansari, N. H. Yarkandi, E. Danish, M. D. Y. Oteef, and M. Cohelan, "Photocatalytic Degradation of Methyl Tert-Butyl Ether (MTBE): A Review," Adv. Env. Res., Vol. 3 No. 1, pp. 11-28, 2014.

[2] M. N. Siddiqui and M. A. Gondal, "Nanocatalyst Support of Laser-Induced Photocatalytic Degradation of MTBE," J. Environ. Sci., Vol 49, pp. 52-58, 2014.

[3] R. L. Zhang, G. Q. Huang, J. Y. Lian, and X. G. Li, "Degradation of MBTE and TBA by a New Isolate from MTBE Contaminated Soil," J. Environ. Sci., Vol. 19, pp. 1120-1124, 2007.

[4] I. Levchuk, A. Bhatnagar, M. Sillanpää, "Overview of Technologies for Removal of Methyl Tert-Butyl Ether (MTBE) from Water," Sci. Total Env., Vol. 476-477, pp. 415-433, 2014.

[5] P. Roslev, T. Lentz, and M. Hesselsoe, "Microbial Toxicity of Methyl Tert-Butyl Ether (MTBE) Determined with Fluorescent and Luminescent Bioassays," Chemosphere, Vol. 120, pp. 284-291, 2014.

[6] L. L. P. Lim and R. Lynch, "Hydraulic Performance of a Proposed In Situ Photocatalytic Reactor for Degradation of MTBE in Water," Chemosphere, Vol. 82, No. 4, pp. 613-620, 2011.

[7] L. L. P. Lim and R. J. Lynch, "In Situ Photocatalytic Remediation of MTBE Contaminated Water: Effects of Organics and Inorganics," Appl. Catal. A: General, Vol. 394, No. 1-2, pp. 52-61, 2011.

[8] Z. S. Seddigi, A. Bumajdad, S. P. Ansari, S. A. Ahmed, E. Y. Danish, N. H. Yarkandi, et al., "Preparation and Characterization of Pd Doped Ceria-ZnO Nanocomposite Catalyst for Methyl Tert-Butyl Ether (MTBE) Photo-Degradation," J. Hazard Mater., Vol. 264, pp. 71-78, 2014.

[9] G. Alfonso-Gordillo, C. M. Flores-Ortiz, L. Morales-Barrera, and E. Cristiani-Urbina, "Biodegradation of Methyl Tertiary Butyl Ether (MTBE) by a Microbial Consortium in a Continuous Up-Flow Packed Bed Biofilm Reactor: Kinetic Study, Metabolite Identification and Toxicity Bioassays," PLOS ONE, pp. 1-21, 2016.

[10] S. H. Sharidi, "Development of Visible Light-Active Catalyst for MTBE Removal from Ground Water," M. S. Thesis, KFUPM, 2012.

[11] S. H. Sharidi, H. Sitepu and N. M. AlYami, "Application of Tungsten Oxide (WO3) Catalysts Loaded with Ru and Pt Metals to Remove MTBE from Contaminated Water: A Case of Laboratory-Based Study," IMPACT: International Journal of Research in Engineering & Technology, ISSN (P): 2347-4599; ISSN (E): 2321-8843; Impact Factor (JCC): 3.9074, Vol. 6, Issue 8, Aug 2018, 19-30.

[12] H. Sitepu, B. H. O'Connor, and D. Y. Li, "Comparative Evaluation of the March and Generalized Spherical Harmonic Preferred Orientation Models Using X-ray Diffraction Data for Molybdite and Calcite Powders," J. Appl. Cryst., Vol. 38, No. 1, pp. 158-167, 2005.

[13] H. Sitepu, "Rietveld Phase Analysis of Deposits Formed at Different Locations within Electric Submersible Pumps," Adv. X-ray Anal., Vol. 63, 2020, In print.

[14] H. Sitepu, and R. A. Al-Ghamdi, "Quantitative Phase Analysis of XRD Data of Sludge Deposits from Refineries and Gas Plants by Use of the Rietveld Method," Adv. X-ray Anal., Vol. 62, pp. 45-57, 2019.

[15] T. Degen, M. Sadki, E. Bron, U. König, and G. Nénert, "The HighScore Suite," Powder Diffr., Vol. 29, pp. S13-S18, 2014.

[16] ICDD, "PDF-4+ 2019 (Database)," edited by Dr. Soorya Kabekkodu, International Centre for Diffraction Data, Newtown Square, PA, USA, 2018.

[17] N. V. Y. Scarlett, I. C. Madsen, L. M. D. Cranswick, T. Lwin, E. Groleau, G. Stephenson, M. Aylmore, and N. Agron-Olshina, "Outcomes of the International Union of Crystallography Commission on Powder Diffraction Round Robin on Quantitative Phase Analysis: samples 2, 3, 4, synthetic bauxite, natural granodiorite and pharmaceutical," Journal of Applied Crystallography, Vol. 35, 2002, 383-400.

[18] B. H. O'Connor, D. Y. Li, and H. Sitepu, "Strategies for preferred orientation corrections in X-ray powder diffraction using line intensity ratios," Advances in X-Ray Analysis, Vol. 34, 1991, 409-415.